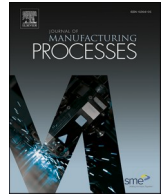




Contents lists available at ScienceDirect

Journal of Manufacturing Processes

journal homepage: www.elsevier.com/locate/manpro

Effect of printing parameters on the electromagnetic shielding efficiency of ABS/carbonaceous-filler composites manufactured via filament fused fabrication

D.P. Schmitz^{a,*}, S. Dul^b, S.D.A.S Ramoa^a, B.G. Soares^c, G.M.O. Barra^a, A. Pegoretti^b

^a Department of Mechanical Engineering, Universidade Federal de Santa Catarina, Florianópolis, SC, Brazil

^b Department of Industrial Engineering, University of Trento, Trento, Italy

^c Department of Metallurgic and Materials Engineering, Universidades Federal do Rio de Janeiro, Rio de Janeiro, RJ, Brazil

ARTICLE INFO

Keywords:

Fused filament fabrication
Electromagnetic interference shielding efficiency
Polymeric composites

ABSTRACT

This work assesses the influence of material composition as well as printing parameters on the electromagnetic interference shielding effectiveness (EMI SE) of polymeric composites based on poly(acrylonitrile-co-butadiene-co-styrene) (ABS) filled with carbon nanotubes (CNT) and/or carbon black (CB), manufactured via fused filament fabrication (FFF). In the study three compositions were analyzed, ABS with 5 wt% of CNT, ABS with 5 wt% of CB, and a hybrid composite with also 5 wt% total of additive but a (75:25) fraction of CNT:CB. The materials properties were evaluated on samples printed in three different growing directions, horizontal concentric (HC), perpendicular concentric (PC) and horizontal at $\pm 45^\circ$ (H45). The electrical conductivity of the printed samples are highly influenced by the CNT presence in the composition, and increased with its incorporation. The electrical conductivity values for ABS with 5 wt% of CB were in the range of 10^{-12} S. cm^{-1} , while for hybrid composite and ABS with 5 wt% of CNT values between 10^{-8} and 10^{-5} S. cm^{-1} were observed. The EMI SE, for all patterns of printed samples, also increased with the increase of CNT amount and layer thickness, with values of around -16 dB for the composite with only CNT sample, and -14 dB for the hybrid sample. The PC pattern shows high anisotropy among the studied samples, presenting the highest EMI SE value for PC when measured horizontally (PC-H) and the lowest value when measured vertically (PC-V). The results obtained in this study show the real potential of applying FFF for the manufacturing of ABS/carbonaceous composites to be use in EMI shielding applications.

Introduction

Studies of additive manufacturing (AM) for producing components with innovative application have grown in the last few years [1–4]. Additive manufacturing is a set of techniques based on building detailed forms layer by layer, and its main advantage is the possibility of creating objects straight from the 3D model, without the need of molds, with efficiency and very little to none material waste. The main steps comprise the following: creating a 3D digital model by computer-aided design (CAD) type software; slicing the model to create the layers to be printed; and finally printing the part with the use of a 3D printer [1,2].

There are several types of AM techniques available on today's market, and their selection will depend specially on the chosen raw material and final application of the printed part [5–7]. Among these techniques,

fused filament fabrication (FFF) has become one of the most commonly used additive manufacturing processes, mainly due to the ease of processing, cheaper equipment and diversity of feedstock materials. This technology uses thermoplastic polymers in the form of filaments as the raw material, being poly(lactic acid) (PLA), poly(acrylonitrile-butadiene-styrene) (ABS), nylon and PETG (glycol-modified polyethylene terephthalate) the most commonly used [8,9]. This technique versatility regarding raw materials allows the use of polymeric composites to manufacture multi-function components for several technological applications, such as, specimens with gradient composition, electrical and thermal conductivity, increased mechanical properties, electromagnetic shielding, among others [10–15]. At the same time, the components quality and properties are not only dependent on the raw material, but also on the printing parameters [3,9,16],

* Corresponding author.

E-mail address: dehschmitz@gmail.com (D.P. Schmitz).

<https://doi.org/10.1016/j.jmpro.2021.02.051>

Received 7 June 2020; Received in revised form 26 February 2021; Accepted 28 February 2021

Available online 15 March 2021

1526-6125/© 2021 The Society of Manufacturing Engineers. Published by Elsevier Ltd. All rights reserved.

which makes its study imperative.

Electromagnetic interference (EMI), caused by radiation or conduction of electromagnetic waves, has increased in recent years due to electronic devices' proliferation, becoming a serious worry. The interference may occur between different equipment or inside a single system, by its components [17,18]. Therefore, several studies have been carried out to develop materials and components to be used as a shield against EMI. The shielding efficiency (EMI SE) of a material depends on several factors, such as, thickness, electrical conductivity and permittivity, and amount of charge carrier. As an alternative to metals, electrically conductive composites based on carbonaceous nanoadditives (carbon nanotubes, carbon black, graphene, graphite, etc.) have shown interesting results [19–22].

The use of the FFF technique for producing components with electrically conductive polymer composites to be applied as an electromagnetic shield has shown great potential [11,23–25]. Prashantha and Roger (2017) studied the application of samples made by PLA filled with 10 wt% of conductive graphene for EMI SE. The authors observed that the electrical conductivity of the filament used as feedstock is higher than the printed samples and that the values vary with the measurement orientation. For EMI SE they obtained samples with values around 16 dB [11]. Ecco et al. (2019) studied the influence of incorporating 6 wt% of graphene nanoplatelets (xGnP) and CNT in the electrical and electromagnetic properties of ABS composites samples. The ABS/CNT samples presented higher electrical conductivity and EMI SE values when compared with the ABS/xGnP samples. The authors also observed that changes in the printing configuration influenced the shielding effectiveness greatly, decreasing from -25 dB to -15 dB for the ABS/CNT samples [23]. Dul et al. (2020) analyzed the influence of mixing xGnP and CNT on the electrical and electromagnetic properties of the studied samples. This study showed EMI SE values of FFF parts between -16 dB to -11 dB [15]. Similar studies were previously performed by our group, which demonstrated the possibility of using the FFF process to produce samples based on composites of ABS with CNT and/or CB, with 3 wt% total of incorporated filler, for electromagnetic shielding application [24]. However, the obtained values for EMI SE were small, not higher than -15 dB for ABS/CNT, which incites the investigation of composites with higher amount of filler, as well as the influence of different printing configuration, such as layer height.

In this study, the influences of the relative ratio of CNT/CB, layer height, printing pattern, and sample anisotropy on the shielding effectiveness of ABS/CNT/CB composites, with total filler amount of 5 wt%, will be analyzed.

Experimental

Materials

Acrylonitrile–butadiene–styrene (ABS) copolymer pellets, grade Cyclocac™ Resin MG47, with specific gravity of 1.04 and MFI (220 °C/10 kgf) of 18 g/10 min, were supplied by Sabic (Brazil). The carbonaceous filler used were: multi-walled carbon nanotubes, grade Nanocyl™ NC7000, supplied by Nanocyl S.A (Belgium); and carbon black, grade PRINTEX XE 2-B, supplied by Orion Engineered Carbon (US).

Experimental methodology

Compounding and filament preparation

Initially the ABS pellets and the filler were dried at 60 °C overnight. The composites were compounded using an internal mixer (Thermo Scientific Haake™, Polylab™ Rheomix 600p) at a temperature of 230 °C, for 15 min at a rotor speed of 60 rpm. Three composites, based on ABS with CNT and CB, were prepared with a fixed filler weight fraction of 5 wt% and CNT/CB ratios of 0/100, 75/25 and 100/0. The compositions were chosen according to previous studies, made by this group [19], about the shielding efficiency of compressed molded samples of

Table 1
Composites formulation.

Composite	Representation	Filler	Formulation (wt%)
ABS/CNT/ CB	(95/0/5)	Carbon black (CB)	ABS (95) / CB (5)
	(95/3.75/ 1.25)	CNT + CB	ABS (95) / CNT (3.75) / CB (1.25)
	(95/5/0)	Carbon nanotube (CNT)	ABS (95) / CNT (5)

ABS with carbonaceous fillers. The aforementioned work showed that the 5 wt% composition displays the best relationship between electromagnetic properties and processability (i.e. melt flow index) for the studied samples. The composites' formulation is detailed in Table 1.

After mixing, all composites were ground by a slow speed granulator (Piovan, model RN 166), to small-sized particles, in order to facilitate a regular feeding of the extruder and insure a homogeneous filament. Before extrusion, the composites were dried overnight at 60 °C. The filaments were produced using a single-screw extruder (Friul Filiere SpA, model Estru 13), with screw diameter of 14 mm and rod die diameter of 2 mm. The extruder has four heating zones that had their temperatures kept at: 100, 200, 220 and 230 °C (from feeding zone to rod die zone). The screw speed was kept at 30 rpm and the collection rate was adjusted to obtain filaments with a diameter of 1.75 ± 0.10 mm.

Printing samples via FFF

The samples were manufactured with a “Next generation” desktop 3D printer by Sharebot (Nibionno, Italy). All patterns were printed with a nozzle of 0.4 mm with temperature of 250 °C, and bed temperature of 110 °C. The printing speed was kept at 40 mm/s and the printing infill at 100 %. Three printing patterns were manufactured for layer height of 0.2 mm under three different build up geometries, i.e. horizontal concentric (HC), perpendicular concentric (PC) and horizontal at $\pm 45^\circ$ (H45). These samples were tested for electrical conductivity and shielding effectiveness. Likewise, two printing patterns were manufactured with a layer height of 0.1 mm: PC and H45 (used only to analyze shielding effectiveness). All samples have a total thickness of 2 mm. A schematic image of all printing patterns is detailed in our previous works [24].

Characterization

Electron microscopy

Filler distribution and nanocomposite morphology of the filaments and the printed samples were studied by field emission gun scanning electron microscopy (FEG-SEM), with a Jeol model JSM-6390LV microscope at an acceleration voltage of 10 kV. The samples were cooled in liquid nitrogen to obtain a cross-section with fragile fracture, and its surface sputtered with a thin layer of gold.

Electrical conductivity

The filaments and the printed samples volume electrical conductivity (σ) were measured in direct current (DC) at room temperature. The specimens were measured by the two-probe method, using a Keithley current source (model 6220) and a Keithley electrometer (model 6517A). Eq. 1 was used to calculate the electrical conductivity for the two-probe method:

$$\sigma = \frac{4w}{\pi R d^2} \quad (1)$$

where, σ is the volume electrical conductivity ($S \cdot cm^{-1}$), R is the materials resistance (Ω), d is the diameter (cm) and w is the thickness (cm).

Electromagnetic interference shielding effectiveness (EMI SE)

The electromagnetic interference shielding effectiveness (EMI SE)

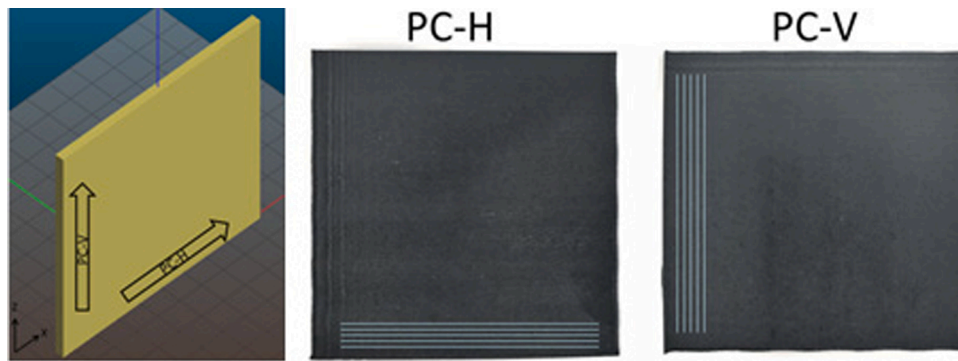


Fig. 1. Placement direction of PC samples in the microwave network analyzer. PC-H for the sample positioned horizontally, and PC-V for the sample positioned vertically, to the printing direction.

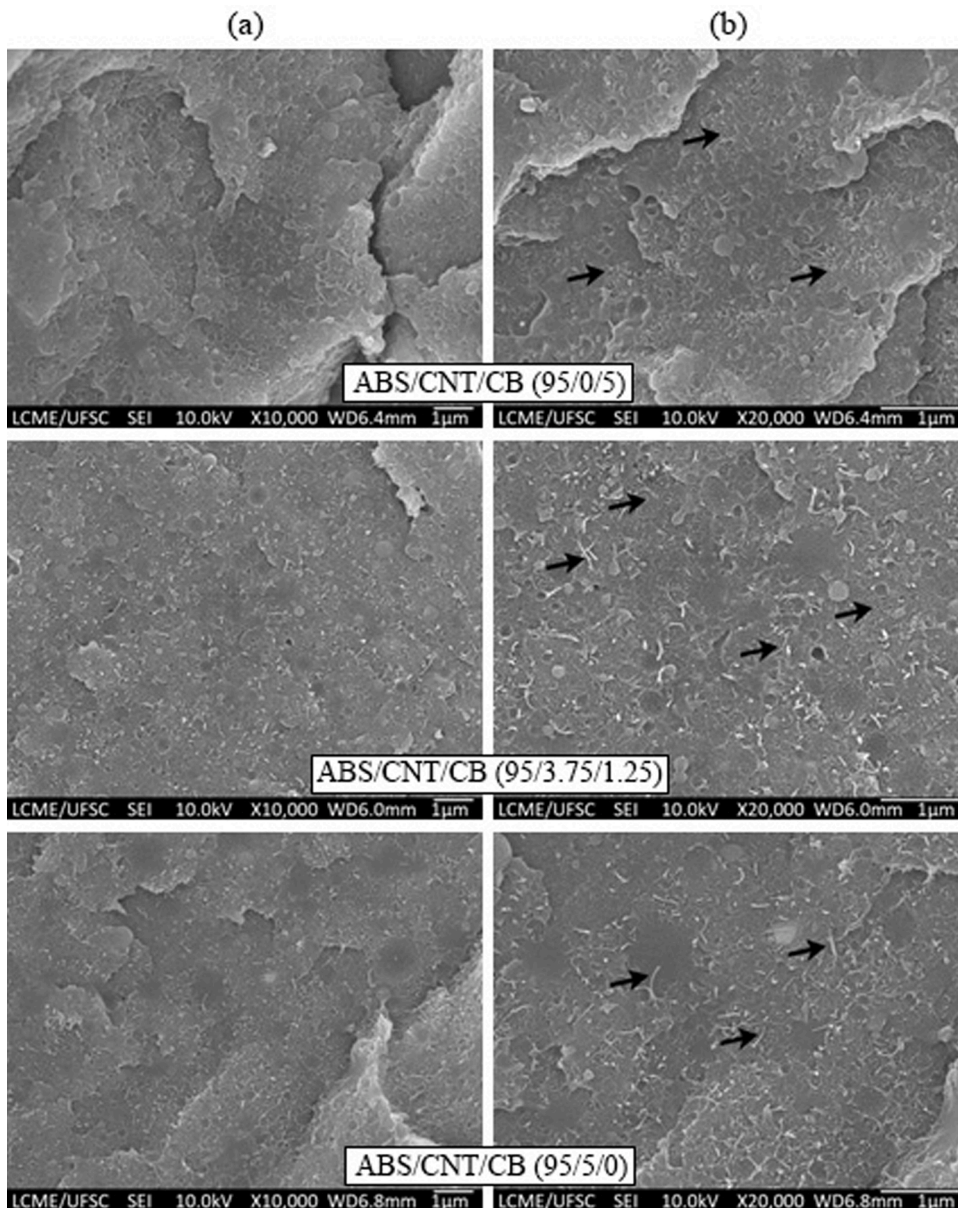


Fig. 2. Fractured surface of ABS/CNT/CB filaments. Magnification: (a) x10000 e (b) x20000. Inserted arrows emphasize the presence of CNT and CB particles.

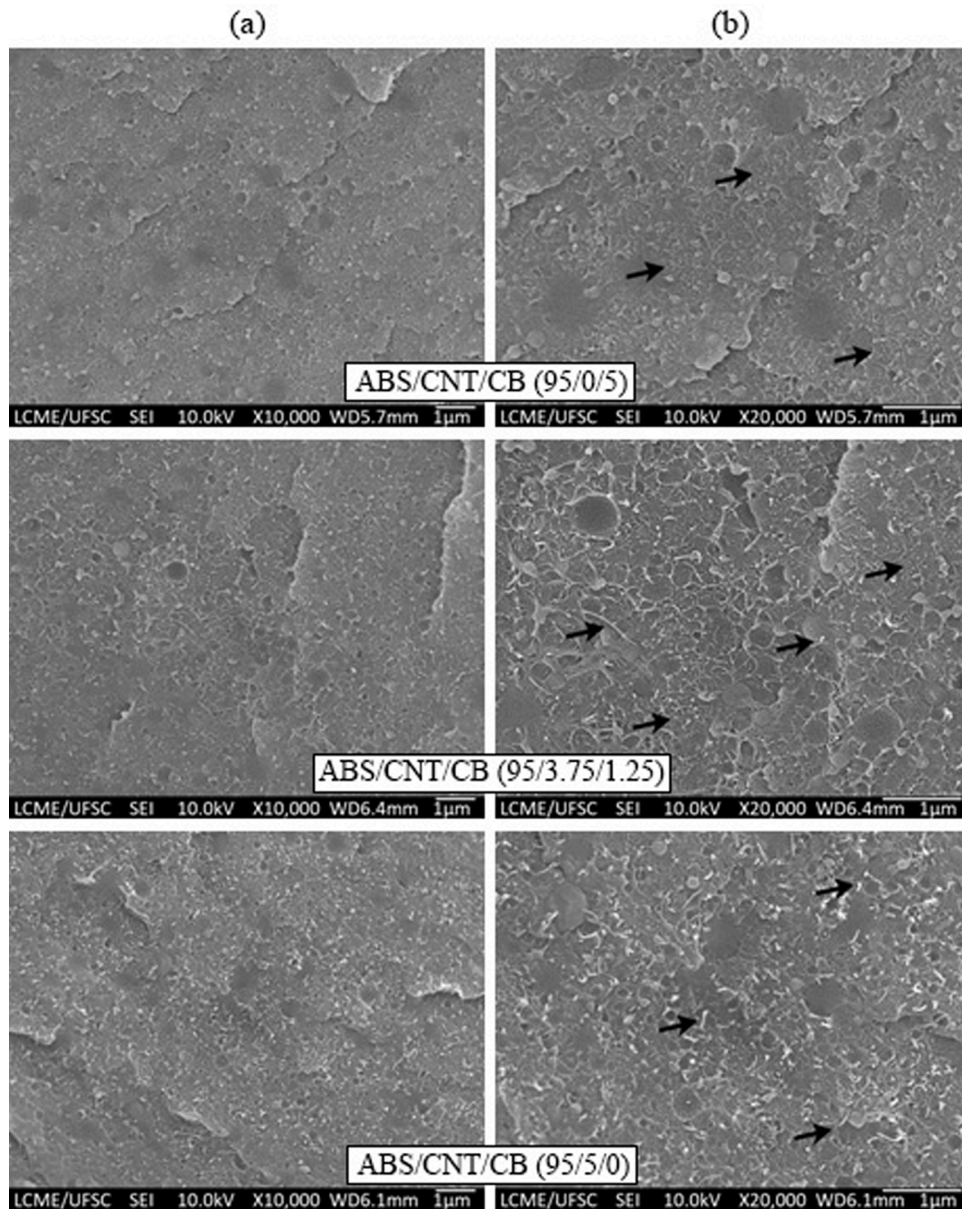


Fig. 3. Fractured surface of ABS/CNT/CB printed sample with a layer height of 0.2 mm. Magnification: (a) x10000 e (b) x20000. Inserted arrows emphasize the presence of CNT and CB particles.

was performed using a N5230C/PNA-L microwave network analyzer (Agilent Co), with a rectangular waveguide, in the X-band microwave frequency range (between 8.2 and 12.4 GHz).

The EMI SE, in dB, was calculated (Eq. 2) through the scattering parameters (S), related to the intensity of the reflected (S_{11} or S_{22}) and transmitted (S_{12} or S_{21}) waves.

$$EMI SE = 10 \log \frac{1}{|S_{12}|^2} = 10 \log \frac{1}{|S_{21}|^2} \quad (2)$$

When an electromagnetic wave interacts with a material, part of it is reflected (R) by the material, part is absorbed (A) and part is transmitted (T). Thus, the sum of a unit of wave (Eq. 3) is illustrated as:

$$R + A + T = 1 \quad (3)$$

With,

$$T = S_{12}^2 = S_{21}^2$$

$$R = S_{11}^2 = S_{22}^2$$

Therefore, the electromagnetic shielding mechanism can be expressed as the sum of the shielding by absorption (SE_a) and the shielding by reflection (SE_r), depending on how the wave interacts with the material. These two components can be calculated according to Eqs 4 and 5.

$$SE_a = 10 \log \log \left(\frac{1-R}{T} \right) \quad (4)$$

$$SE_r = 10 \log \log \left(\frac{1}{1-R} \right) \quad (5)$$

All measurements were repeated for three samples of each build up geometry (PC, H45 and HC). Besides, the EMI SE for the PC samples were analyzed in two orientations, one where the sample is placed as printed (PC-H, positioned horizontally), and the other where the sample is turned to its side (PC-V, positioned vertically), as shown in Fig. 1.

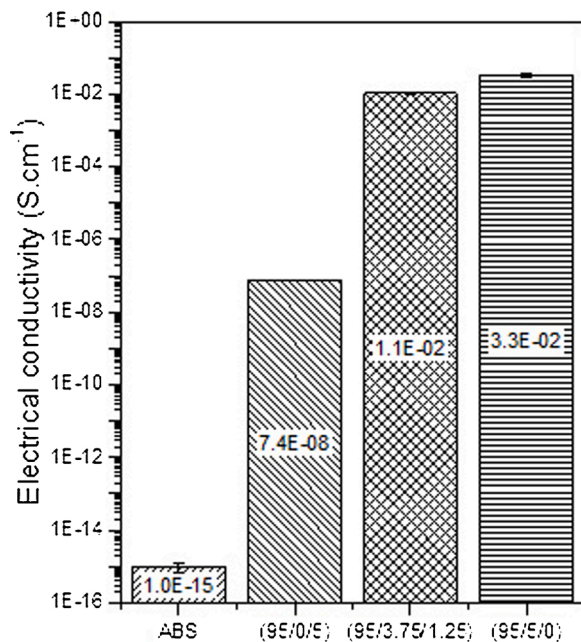


Fig. 4. Electrical conductivity of ABS and composites filaments with 5 wt% total filler.

Results and discussion

Morphology and filler dispersion

Initially, the composites' morphology was analyzed by electrical microscopy. Fig. 2 illustrates the fracture surface of the filaments used as feedstock. For all the composites it is observed that the fillers particles are well dispersed and distributed. Fig. 3 shows the micrograph of the printed samples, which is very similar to the filaments. This indicates that the main influence on the printed samples properties will be related to the printing parameters.

Electrical conductivity

The filaments electrical conductivity is shown in Fig. 4. The electrical conductivity increases with the addition of CNT in the formulation. The composite with only CB presents a value that is 6 orders of magnitude lower than the composites with CNT. These results can be related to the higher aspect ratio and electrical conductivity of the CNT when compared with CB.

To measure the electrical conductivity of the printed samples, the probes were connected to the samples sides with larger areas. Thus, for the PC sample the face in contact with the probes was the XZ, while for the HC and H45 samples were the faces XY. Fig. 5 illustrates the setup for

the measurement, highlighting the direction of the current application (arrow). The same directions were used to measure the samples' EMI SE.

Fig. 6 shows the influence of geometry and type of filler on the electrical conductivity of the ABS/CNT/CB composites with 5 wt% total of filler. In general, the conductivity of 3D-printed samples is lower than that of filaments due to the internal features of FFF samples, which is in agreement to previous research [13]. Also, the electrical conductivity of the printed samples increases with the increasing amount of CNT incorporated. The increase of the composites electrical conductivity in relation to the matrix was 4 orders of magnitude for a composition with only CB (95/0/5). Meanwhile, for composites with CNT incorporated (95/3.75/1.25 and 95/5/0), the increase was 7 orders for PC and 5 for HC and H45. According to these results, it can be inferred that the samples conductivity is also dependent on their printing orientation. The samples manufactured in the PC direction presented electrical conductivity two orders of magnitude higher than the other configurations for all compositions containing CNT.

Considering the arrangement of the electrodes (terminals) for the electrical conductivity measurement, one of the reasons for the conductivity variation may be due to the way the electric current is conducted in the samples. In the PC orientation the electrical current applied by the two terminals follows in the same direction as the filament printing, so the current flows through the filament. However, in the HC and H45 orientations, the electrodes are arranged so that they are separated by the sample layers, which results in the need for current to pass between the filament surfaces, which may interfere in the current conduction. It is also worth noticing that the values for electrical conductivity for the printed samples are lower than the ones for the filaments used as feedstock, as well as the ones for ABS/CNT and or ABS/CB reported in the literature for compressed molded samples [19]. This behavior can be attributed to the large number of defects, mostly voids, and the increased surface area between filaments, which hinder the applied current flow.

Electromagnetic shielding effectiveness (EMI SE)

The average shielding efficiency of ABS and ABS/CNT/CB samples with 5% total weight of additive, with different print orientations and layer height of 0.2 mm, is shown in Fig. 7. It is important to remember that the electromagnetic wave are passing through samples HC and H45 in the Z direction and sample PC in the Y direction, as shown in Fig. 5. Also, the PC samples were measured horizontally (PC-H) and vertically (PC-V), as shown in Fig. 1.

The EMI SE is dependent on composition, electrical conductivity, and print orientation. For all samples, as shown for electrical conductivity, the total average EMI SE of the composites increases with the incorporation of CNT in the matrix. This behavior is related to the fact that CNT presents higher electrical conductivity and aspect ratio than CB, which facilitates the interaction between the electromagnetic wave and the additive.

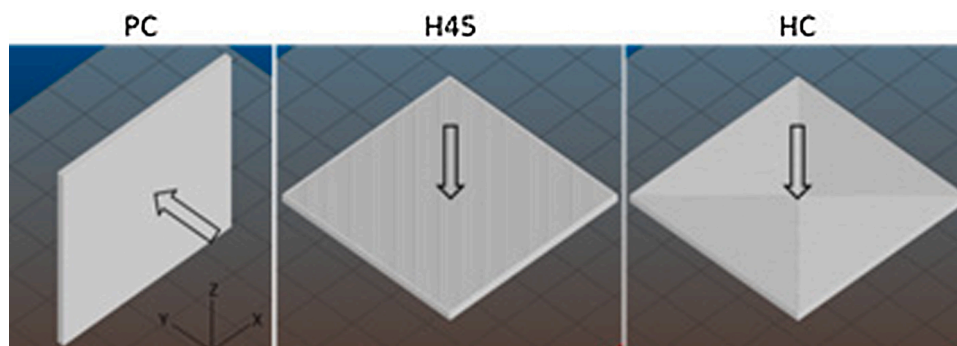


Fig. 5. Direction of current application and electromagnetic wave flow for printed samples.

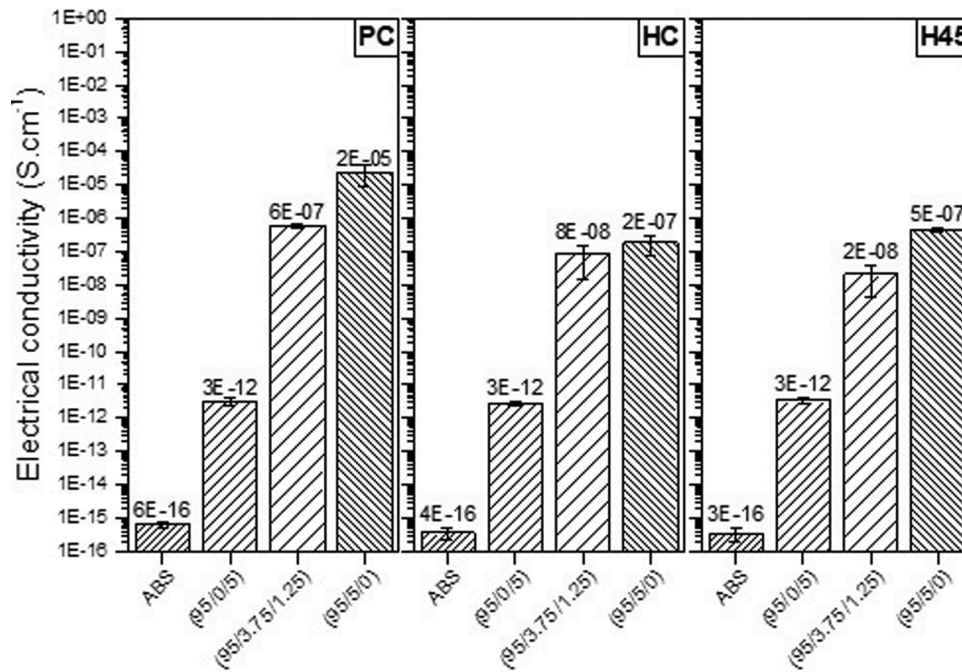


Fig. 6. Electrical conductivity of printed ABS and ABS/CNT/CB with 5 wt% and layer height of 0.2 mm.

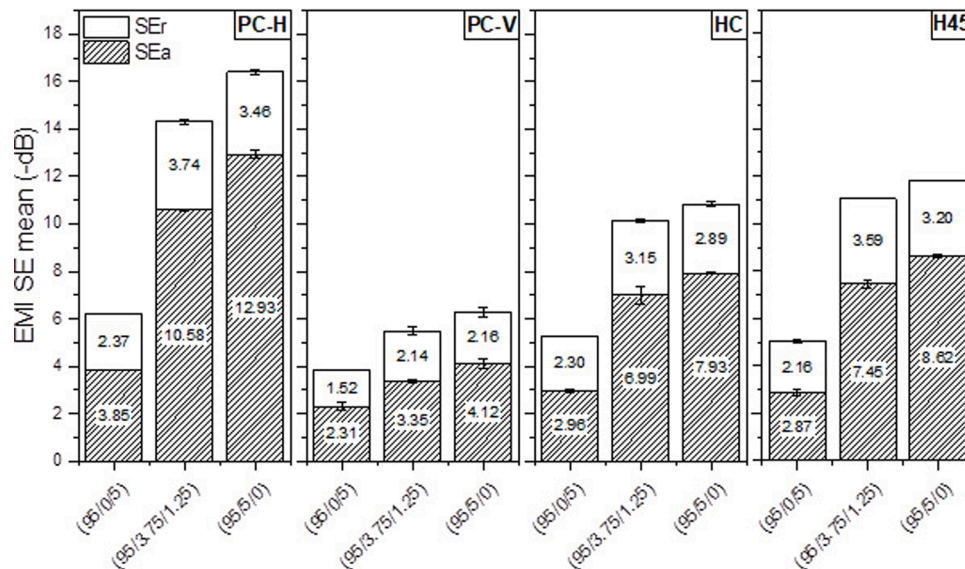


Fig. 7. EMI SE mean of FFF composites ABS/CNT/CB samples with 5 wt% total of filler and layer height of 0.2 mm.

The EMI SE of samples produced in the HC and H45 orientation showed similar behavior, with values of around -11 dB for compositions with (95/3.75/1.25) and (95/5/0) wt%, and -5 dB for the (95/0/5) wt% composition. As for the PC samples, it is interesting to note that the values change drastically when the measurement orientation is altered. The PC-H showed higher results for all compositions, with EMI SE values of approximately -16 dB for (95/3.75/1.25) and (95/5/0) wt%, and -6 dB for (95/0/5) wt%. However, the PC-V showed the worst result, with values of EMI SE barely reaching -6 dB for all compositions. These results show that, although the PC can have good results, it is also highly anisotropic, which can hinder the application of the component. Meanwhile, the HC and H45 show average values, between PC-H and PC-V, but do not have the orientation problem.

The obtained values, presented on Fig. 7, are relatively lower when compared with composites of similar composition, but prepared by

processing that result in dense samples, like compression and injection molding. For the same amount of CNT, a dense sample produced via compression molding showed an EMI SE of around -45 dB [19]. This difference is related to the presence of defects, inherent to the FFF process, especially porous.

Fig. 8 shows the EMI SE results for PC-H, PC-V and H45 with layer size of 0.1 mm. As it can be seen, the decrease in layer height, from 0.2 mm to 0.1 mm, resulted in the reduction of the shielding efficiency. The expectation was that the increase of the total number of layers, for the same thickness, would improve the results due to the increase of contact surface to interact with the electromagnetic wave. However, with the change in this parameter, the amount of voids in the sample increased, which caused the decline of EMI SE values. This behavior was shown by all samples, but with less impact on the H45 samples.

The dependence between the constructive parameters and the

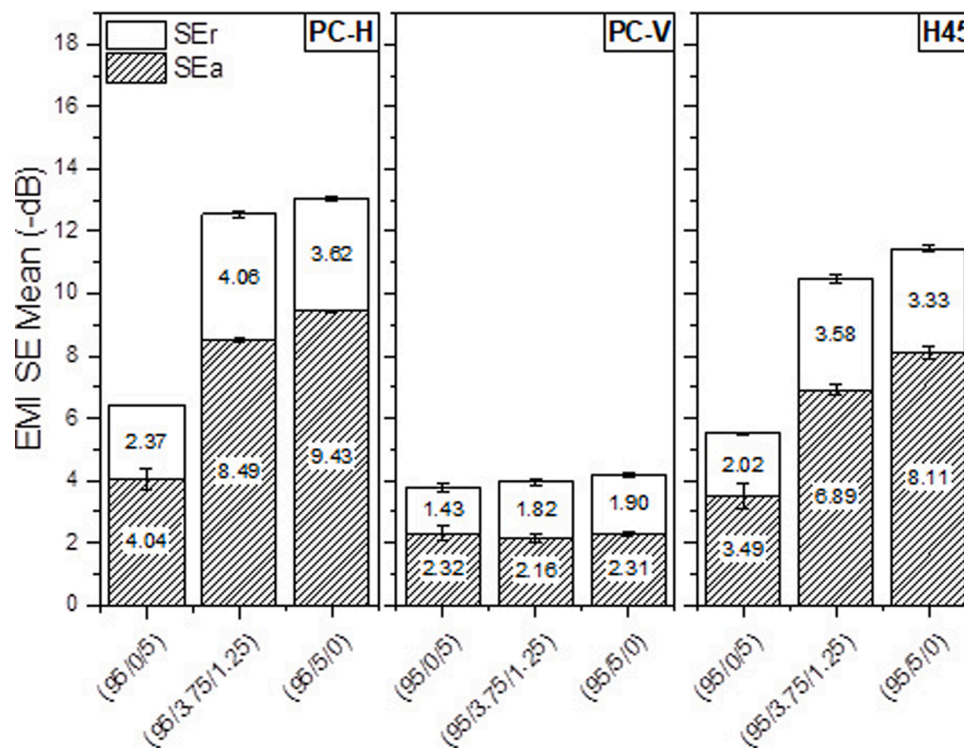


Fig. 8. EMI SE mean of FFF composites ABS/CNT/CB samples with 5 wt% total of filler and layer height of 0.1 mm.

electromagnetic shielding was also analyzed by Viskadourakis et al. (2017) [26]. In their study the authors observed that changing the sample surface texture, in this case adding pyramids on an initially flat surface, results in a significant increase in the EMI SE of the samples. These results demonstrate the importance, and necessity, of studying the components geometry in order to obtain the one with the best properties.

Conclusions

Filaments of ABS/CNT/CB composites were successfully prepared by a single-screw extruder and used as raw material for the FFF process. Three composites were obtained: ABS with 5 wt% of CNT; ABS with 5 wt % of CB; and ABS with 3.75 wt% of CNT and 1.25 wt% of CB. The composites were printed with different patterns (PC, H45 and HC), but same shape and thickness. The influence of composition and printing pattern on electrical conductivity and shielding effectiveness was studied.

The SEM images of the filaments showed the nanoadditives homogeneously dispersed and distributed in the composites matrix, for all compositions. The electrical conductivity, for the filaments and all printing patterns, increased with increasing amounts of CNT. The filaments with CNT in their compositions showed electrical conductivity 6 orders of magnitude higher than the ones with only CB. Among the printed samples, the biggest variance was presented by the PC pattern, with values increasing at least 5 orders of magnitude when CNT was incorporated.

A similar behavior was exhibited by shielding effectiveness, related to the composition. However, the printing pattern seemed to have higher influence on the EMI SE values. For all the samples, the PC-H pattern presented the highest EMI SE value, around -16 dB for samples with layer height of 2 mm. At the same time, the PC-V showed the lowest. This discrepancy in behavior can be related to the pattern considerable anisotropy, which isn't presented by the HC and H45 specimens. Another printing parameter with impact in the EMI SE values is the layer's height. A smaller layer height (0.1 mm) resulted in worse

EMI SE results, due to the presence of opening between the deposited filaments. This defect could be resolved by changing the printing nozzle to a bigger one, which could assure better material flow and that the deposited filaments would be closer together, preventing the opening's formation.

The results of EMI SE found in this study are in accordance with other works in the literature about carbonaceous based polymer composites, and show the real potential of applying FFF to manufacture specimens of ABS/Carbonaceous composites to be use in shielding applications.

Funding

This work was financially supported by the Brazilian research foundations: Conselho Nacional de Desenvolvimento Científico e Tecnológico (CNPq), and Coordenação de Aperfeiçoamento de Pessoal de Ensino Superior (CAPES).

Declaration of Competing Interest

The authors report no declarations of interest.

Acknowledgements

The authors also gratefully acknowledge the Central Electron Microscopy Laboratory of Universidade Federal de Santa Catarina (LCME-UFSC) for the FEG-SEM images.

References

- [1] Tofail SAM, Koumoulos EP, Bandyopadhyay A, Bose S, O'Donoghue L, Charitidis C. Additive manufacturing: scientific and technological challenges, market uptake and opportunities. *Mater Today* 2018;21:22–37. <https://doi.org/10.1016/j.mattod.2017.07.001>.
- [2] Rayna T, Striukova L. From rapid prototyping to home fabrication: how 3D printing is changing business model innovation. *Technol Forecast Soc Change* 2015;102: 214–24. <https://doi.org/10.1016/j.techfore.2015.07.023>.

- [3] Bähr F, Westkämper E. Correlations between influencing parameters and quality properties of components produced by fused deposition modeling. *Procedia Cirp* 2018;72:1214–9. <https://doi.org/10.1016/j.procir.2018.03.048>.
- [4] hizari K, Arjmand M, Liu Z, Sundararaj U, Therriault D. Three-dimensional printing of highly conductive polymer nanocomposites for EMI shielding applications. *Mater Today Commun* 2017;11:112–8. <https://doi.org/10.1016/j.mtcomm.2017.02.006>.
- [5] Redwood B, Schöffner F, Garret B. *The 3D printing handbook*. 3D Hubs; 2017. p. 347.
- [6] Wang X, Jiang M, Zhou Z, Gou J, Hui D. 3D printing of polymer matrix composites: a review and prospective. *Compos Part B Eng* 2017;110:442–58. <https://doi.org/10.1016/j.compositesb.2016.11.034>.
- [7] de Leon AC, Chen Q, Palaganas NB, Palaganas JO, Manapat J, Advincula RC. High performance polymer nanocomposites for additive manufacturing applications. *React Funct Polym* 2016;103:141–55. <https://doi.org/10.1016/j.reactfunctpolym.2016.04.010>.
- [8] Stansbury JW, Idacavage MJ. 3D printing with polymers: challenges among expanding options and opportunities. *Dent Mater* 2015;32:1–11. <https://doi.org/10.1016/j.dental.2015.09.018>.
- [9] Yadav D, Chhabra D, Kumar Garg R, Ahlawat A, Phogat A. Optimization of FDM 3D printing process parameters for multi-material using artificial neural network. *Mater Today Proc* 2020;21:1583–91. <https://doi.org/10.1016/j.matpr.2019.11.225>.
- [10] Heidari-Rarani M, Rafiee-Afarani M, Zahedi AM. Mechanical characterization of FDM 3D printing of continuous carbon fiber reinforced PLA composites. *Compos Part B Eng* 2019;175:107147. <https://doi.org/10.1016/j.compositesb.2019.107147>.
- [11] Prashantha K, Roger F. Multifunctional properties of 3D printed poly(lactic acid)/graphene nanocomposites by fused deposition modeling. *J Macromol Sci Part A Pure Appl Chem* 2017;54:24–9. <https://doi.org/10.1080/10601325.2017.1250311>.
- [12] Sezer HK, Eren O. FDM 3D printing of MWCNT re-inforced ABS nano-composite parts with enhanced mechanical and electrical properties. *J Manuf Process* 2019; 37:339–47. <https://doi.org/10.1016/j.jmapro.2018.12.004>.
- [13] Dul S, Fambri L, Pegoretti A. Filaments production and fused deposition modelling of ABS/carbon nanotubes composites. *Nanomaterials* 2018;8. <https://doi.org/10.3390/nano8010049>.
- [14] Dorigato A, Moretti V, Dul S, Unterberger SH, Pegoretti A. Electrically conductive nanocomposites for fused deposition modelling. *Synth Met* 2017;226:7–14. <https://doi.org/10.1016/j.synthmet.2017.01.009>.
- [15] Dul S, Ecco LG, Pegoretti A, Fambri L. Graphene/carbon nanotube hybrid nanocomposites: effect of compression molding and fused filament fabrication on properties. *Polymers (Basel)* 2020;12. <https://doi.org/10.3390/POLYM12010101>.
- [16] Chacón JM, Caminero MA, García-Plaza E, Núñez PJ. Additive manufacturing of PLA structures using fused deposition modelling: effect of process parameters on mechanical properties and their optimal selection. *Mater Des* 2017;124:143–57. <https://doi.org/10.1016/j.matdes.2017.03.065>.
- [17] Tong XC. *Advanced materials and design for electromagnetic interference shielding*. CRC Press; 2008.
- [18] Kaur M, Kakar S, Mandal D. Electromagnetic interference. 2011 3rd Int Conf Electron Comput Technol, 4; 2011. p. 1–5. <https://doi.org/10.1109/ICECTECH.2011.5941844>.
- [19] Schmitz DP, Silva TI, SDAS Ramoa, Barra GMO, Pegoretti A, Soares BG. Hybrid composites of ABS with carbonaceous fillers for electromagnetic shielding applications. *J Appl Polym Sci* 2018;135:12–5. <https://doi.org/10.1002/app.46546>.
- [20] Kuester S, Demarquette NR, Ferreira JC, Soares BG, Barra GMO. Hybrid nanocomposites of thermoplastic elastomer and carbon nanoadditives for electromagnetic shielding. *Eur Polym J* 2017;88:328–39. <https://doi.org/10.1016/j.eurpolymj.2017.01.023>.
- [21] Electrical Al-Saleh MH. EMI shielding and tensile properties of PP/PE blends filled with GNP:CNT hybrid nanofiller. *Synth Met* 2016;217:322–30. <https://doi.org/10.1016/j.synthmet.2016.04.023>.
- [22] Tiwari SK, Mishra J, Hatui G, Nayak GC. Conductive polymer composites based on carbon nanomaterials. In: Kumar V, Kalia S, Swart HC, editors. *Conduct. Polym. Hybrids*. Cham: Springer International Publishing; 2017. p. 117–42. https://doi.org/10.1007/978-3-319-46458-9_4.
- [23] Ecco LG, Dul S, Schmitz DP, Barra GM de O, Soares BG, Fambri L, et al. Rapid prototyping of efficient electromagnetic interference shielding polymer composites via fused deposition modeling. *Appl Sci (Basel)* 2018;9. <https://doi.org/10.3390/app9010037>.
- [24] Schmitz DP, Ecco LG, Dul S, Pereira ECL, Soares BG, Barra GMO, et al. Electromagnetic interference shielding effectiveness of ABS carbon-based composites manufactured via fused deposition modelling. *Mater Today Commun* 2018;15:70–80. <https://doi.org/10.1016/j.mtcomm.2018.02.034>.
- [25] Paddubskaya A, Valynets N, Kuzhir P, Batrakov K, Maksimenko S, Kotsilkova R, et al. Electromagnetic and thermal properties of three-dimensional printed multilayered nano-carbon/poly(lactic) acid structures. *J Appl Phys* 2016;119. <https://doi.org/10.1063/1.4945576>.
- [26] Viskadourakis Z, Vasilopoulos KC, Economou EN, Soukoulis CM, Kenanakis G. Electromagnetic shielding effectiveness of 3D printed polymer composites. *Appl Phys A* 2017;123:736. <https://doi.org/10.1007/s00339-017-1353-z>.